ELSEVIER

Nuclear Instruments and Methods in Physics Research B 143 (1998) 188–194

NIM B
Beam Interactions with Materials & Atoms

New source of ultra-cold positron and electron beams

C. Kurz, S.J. Gilbert, R.G. Greaves, C.M. Surko *

Dept. of Physics, University of California San Diego, 9500 Gilman Drive, La Jolla, CA 92093-0319, USA

Received 29 October 1997

Abstract

We have developed a new and versatile source of cold ($\Delta E \approx 0.018$ eV), low-energy ($E \approx 0 - 9$ eV), magnetized positrons and electrons. Particles are extracted from thermalized, room-temperature, single species plasmas confined in a Penning trap. Typically, the trap contains from 10^7 to 10^9 particles, which can be released either in the form of a quasi steady-state beam or as a pulsed beam. Of the order of 100 pulses of 10^5 positrons, each 10 μs in duration, have been achieved. Size, duration and frequency of pulses within a pulse train are easily variable over a wide range. Cold quasi steady-state electron beams with a diameter of ≈3 mm have also been achieved. Limited only by the total charge contained in the trap, electron currents of 0.1 μA for several milliseconds have been generated routinely. This source represents a combination of attractive features not previously available using any single technique.

PACS: 41.75Fr; 41.75.-i; 52.25.Wz
Keywords: Nonneutral plasmas; Beams; Positrons; Electrons; Monoenergetic; Pulsed

1. Introduction

This paper describes a new and versatile source of high-intensity, cold positrons and electrons. Recently, we introduced the concept of using room-temperature plasmas stored in a Penning trap as a source for cold particle beams [1]. We applied this technique to the production of pulsed and steady-state positron beams and mentioned the possibility of generating electron beams in the same manner. Since then, we have successfully applied this technique to electrons and made several improvements. The aim of the present paper is to discuss the general technique as well as its application to both positron and electron beams.

There are numerous potential applications for bright sources of slow and cold positrons. Examples include material surface characterization, such as defect depth profiling, positron and positronium gas scattering, and annihilation studies [2,3]. Furthermore, many applications of positron beams, such as time-of-flight measurements, positron lifetime experiments, and time tagging, require pulses of positrons. One advantage of pulsed, as compared with steady-state beams, lies in the potential for greatly enhanced signal-to-

* Corresponding author.

0168-583X/98/$19.00
PII: S0168-583X(97)00935-X

noise ratios in a variety of applications. While several techniques to create pulsed positron beams have been discussed previously [4–6], many of these techniques have disadvantages. One example is the degrading of the perpendicular and/or parallel energy spread in order to achieve pulse compression.

There are several possible approaches to generate slow positron beams [2,7]. The positrons originate from either a radioactive source or from a particle accelerator, but in either case they must be slowed from initial energies of several hundred keV to energies in the electron Volt range before beam formation and handling becomes practical. At present this is accomplished most effectively using a solid-state moderating material [2,8–10]. In general, positrons emerge from the moderator with an energy of several electron Volts and an energy spread in the range 0.3–2 eV, although some methods have described to reduce this energy spread by as much as an order of magnitude [11,12]. Another interesting scheme has been proposed which utilizes laser cooled Be^+ ions at a temperature of 10 mK to cool positrons [13].

We have previously developed a technique to trap, store, and manipulate positron plasmas in a Penning–Malmberg trap [14]. Fig. 1 shows a schematic diagram of the experiment. A more detailed description of the apparatus can be found in Ref.

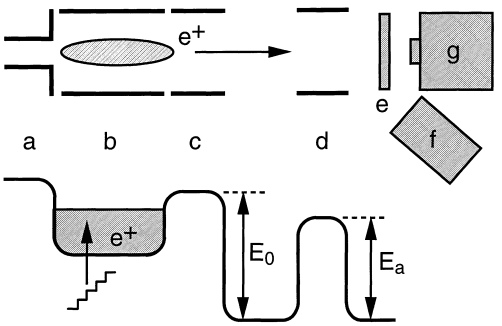

Fig. 1. Schematic diagram of the experiment. The electrodes are shown schematically in the upper diagram. Below, the solid line represents the potentials applied to the electrodes: (a) entrance gate; (b) dump electrode; (c) exit gate; (d) energy analyzer; (e) accelerating grids and phosphor screen; (f) NaI gamma-ray detector; (g) CCD camera. The energies E_0 and E_a are the electrostatic potentials of the exit gate electrode and the energy analyzer, respectively.

[15]. The radial density variations and temporal evolution of the beam profile are analyzed using a CCD camera, viewing a phosphor screen located behind the energy analyzer (shown in Fig. 1). Particles are accelerated to 8 keV before being imaged on the screen. For positrons, a 3-inch NaI(Tl) γ-ray detector provides measurements of particle fluxes. Electron fluxes are sufficiently large to be measured by a standard current-to-voltage amplifier connected to a collection plate.

2. Positron beams

In the case of positron plasmas, a 40-mCi ^{22}Na source provides a flux of fast positrons, which are slowed to an energy of about 2 eV by a solid Ne moderator [9]. The slow positrons are then guided magnetically into a multi-stage Penning trap, where they cool to room temperature by inelastic collisions with nitrogen buffer gas. Collisional cooling on nitrogen has the advantage of increasing the phase–space density of the particles without the losses usually associated with a remoderation stage [16]. The axial magnetic field in the trap is 1 kG.

Positrons have a lifetime of approximately 50 s in the presence of the buffer gas (10^{-7} Torr). If the buffer gas is evacuated, the lifetime is 2 h at the base pressure of the device (5×10^{-10} Torr). An attractive feature of the positron trap is its ability to capture a large fraction ($\approx 30\%$) of the moderated positron beam. For a 40-mCi source, this gives a positron filling rate of $\sim 1 \times 10^6$ s^{-1}. In the experiments described here, positrons were filled for 10 s, resulting in about 10^7 positrons in the trap. Because the fill time is much shorter than the 50-s positron lifetime, the loss of captured positrons during the filling phase is small. The positrons are then dumped in a few milliseconds, so that in this mode of operation, the duty cycle for accumulation is close to unity. Thus, the average throughput is about 1×10^6 positrons per second.

After a positron plasma has been accumulated in the trap, a pulsed positron beam is generated by applying incremental voltage steps to the dump electrode (labeled "b" in Fig. 1), with each increase in voltage ejecting a fraction of the stored

positrons. During this process, the entrance gate ("a") is placed 1 V above the exit gate ("c") to ensure that the positrons leave the trap via the exit gate. The energy of the positron pulses is set by the potential of the exit gate electrode. In order to achieve a narrow energy spread, it is important that the steps in the dump voltage are small compared to the plasma space charge, otherwise collective phenomena can be excited in the charge cloud, which can degrade the achievable energy resolution [17,18]. Using the central electrode to dump small fractions of the plasma, the energy of the released positrons is kept the same for all pulses and is determined solely by the potential of the exit gate.

Fig. 2(a) depicts a pulse train obtained by applying equal-amplitude voltage steps to the dump electrode. For approximately the first 30% of the pulses in the train, the pulse height increases and then stays constant for the remainder of the pulses. The envelope of the pulse train is highly repeatable and unaffected by the number of pulses contained in it. The time-integrated amount of charge dumped from the trap depends only on the dump voltage. By adjusting the size of voltage steps between each pulse, it is possible to compensate for variations in pulse height and achieve a longer flat-topped region. The envelope of the pulse train produced with constant height steps in the dump voltage (e.g., shown in Fig. 2(a)) was used to readjust the dump waveform, and the result is shown in Fig. 2(b). To ensure that all particles with energies greater than the exit gate potential have sufficient time to leave the trap, we apply each voltage step for >15 μs, which is longer than the axial bounce time in the trap ($\tau_b \approx 6$ μs). Pulse durations less than τ_b can be produced by increasing the dump electrode potential for a time shorter than τ_b before returning it to a lower value. This latter protocol produces shorter pulses with a corresponding reduction in the number of positrons per pulse.

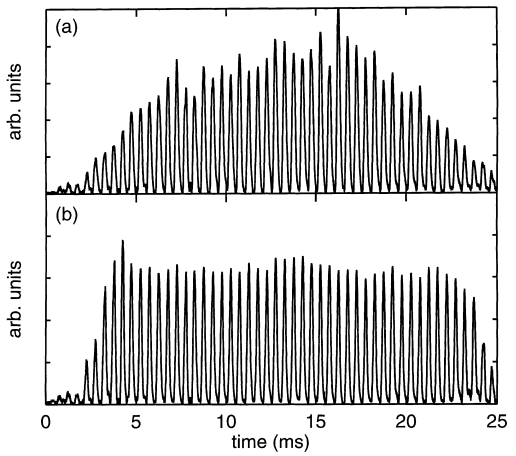

Fig. 2. A pulse train of 60 pulses, each consisting of approximately 10^5 positrons, illustrating the ramp-up, flat-top and terminal phases of the pulse envelope, which is independent of the specific number of pulses: (a) corresponds to equal size steps in the dump voltage; (b) an adapted step size was used to correct for unequal pulse amplitudes. The energy distribution shown in Fig. 3 was obtained for a pulse at the beginning of the flat-top portion of a beam with a similar envelope.

Using a CCD camera, we imaged the radial structure of the pulses, obtaining a size of about 2 cm full width at half maximum (FWHM), roughly equal to the measured plasma size. This is representative of the first 75% of the pulse train. Thereafter, the profiles broaden and become hollow for the last few pulses.

Positron beams with a well-defined energy are of primary importance for many applications. Room-temperature plasmas in the trap will equilibrate to an energy spread corresponding to $\frac{1}{2}kT$ per degree of freedom. In a previous experiment we have shown that the perpendicular energy spread of the plasma is not affected by the dumping process and remains at the room-temperature value [15].

In the regime where the steps in the potential of the dump electrode are small compared to the plasma space charge, the axial pulse energy spread is not affected significantly by the step size or the position of the pulse in the pulse train. Contributing factors to the axial energy spread include the radial variation of the exit gate potential across the plasma width, collective plasma effects [17], and electrical noise on the electrodes. The axial energy spread varies little over pulses in a pulse train.

The axial energy distribution of a pulse taken at the beginning of the flat-topped portion of the pulse envelope is shown in Fig. 3. The number of positrons reaching the energy analyzer (cf.

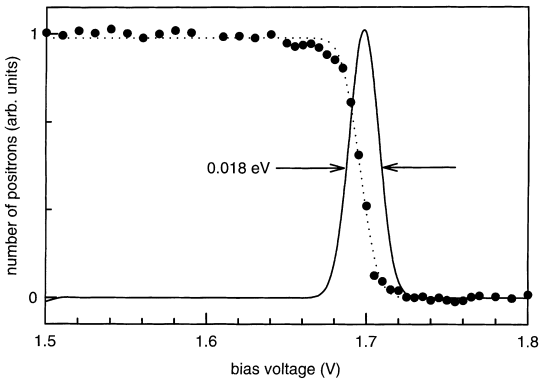

Fig. 3. Energy distribution of a pulse. Filled circles are measured data, and the dashed line is an error function fit to the data. The solid line, which represents the energy distribution, is the derivative of the fit.

Fig. 1) is plotted as a function of analyzer voltage, with the exit gate electrode set at 2 V and a step size of the dump electrode of 37 mV. An error function is fitted to the data and indicates a pulse centroid energy of 1.69 eV, with an energy spread of 0.018 eV FWHM. We attribute the difference of about 0.3 eV between the measured positron energy and the applied exit gate potential to a combination of contact potentials and the radial potential gradient in the trap. A lower limit of the beam energy is expected to be the axial temperature spread of the beam. The highest beam energy used in this experiment was 9 eV, but this was limited only by the maximum output voltage of the digital-to-analog voltage converters.

In practice, the pulse repetition frequency is limited at the lower end by the positron lifetime ($\approx$2 h after evacuation of the buffer gas) and at the high end by the positron bounce time. Pulse amplitudes will be inversely proportional to the number of pulses in the pulse train. However, if small energy spreads are desired, it is necessary to operate in the limit where each step in dump voltage is small compared to the plasma space charge.

We have also created quasi steady-state positron beams of 0.5 s duration with a current of 0.8 pA. This was done by raising the dump voltage continuously over a time scale much longer than the particle bounce time. The beam energy spread in this case was 0.017 eV FWHM, which is comparable to that of the pulsed positron beam.

We are aware of one other report of a Penning trap used as a pulsed source of positrons [19]. Positrons from a LINAC, were captured in a Penning trap and then extracted by applying voltage pulses to the exit gate. However, in this case, no attempt was made to achieve a well-defined beam energy or narrow energy spread.

Brightness is an important figure of merit for beam sources. Use of the positron trap and a buffer gas to cool the positrons increases their phase space density, and hence the beam brightness, without significant loss of beam intensity. The brightness of our pulsed positron beam is $1 \times 10^9\ s^{-1}\ rad^{-2}\ mm^2\ eV^{-1}$, which is significantly higher than the brightness reported for a steady state positron beam with two remoderation stages [2]. In principle, compressing the stored plasma radially by applying an azimuthally rotating electric field to segmented electrodes surrounding the plasma (cf. [20]) or using a source of positrons at cryogenic temperature could enhance the brightness even further.

3. Electron beam

A conventional hot-cathode electron gun yields electron beams with an energy spread typically corresponding to several times the cathode temperature ($\approx$0.5 eV). Electron guns optimized for low energy spreads ($\Delta E \approx 0.2$ eV at a current of several microamps) have been described (e.g., Ref. [21]). However, their operation in a magnetic field environment has not been tested, and the design described in Ref. [21] cannot be used in a magnetic field without modifications. The energy resolution of a primary electron beam can be improved by energy filters of various designs, such as $E \times B$ filters, Wien filters, spherical deflectors, etc. A general discussion of electron monochromator designs in non-magnetized beams shows that 0.3 μA of beam current presents an upper limit, if the energy uncertainty is to remain below 0.1 eV [22].

There are other processes which can produce electrons of well defined energies. For example, a synchrotron photo-ionization technique has been

described, capable of producing electron beams with an energy uncertainty of about 3.5 meV. However, the achievable beam currents are low (of the order of 10^{-12} A).

It is possible to generate well-defined, accurately controllable, and cold steady-state or pulsed electron beams, by extracting electrons from a stored plasma, in a manner similar to that described above for positrons. From a reservoir of 3×10^9 electrons (i.e. 4.8×10^{-10} Coulombs) a beam of, for example, 0.1 μA can be extracted lasting 4.8 ms.

For the electron experiments, we use a commercial dispenser-type cathode with a 2.9 mm aperture as an electron source to fill the Penning trap. The cathode heater current is set so that an extraction voltage of 0.5 V applied to a grid in front of the cathode results in an emission current of about 2 μA. Filling the trap with electrons is achieved without buffer gas at a base pressure of 5×10^{-9} Torr by creating a confining well of gradually increasing depth. The final well depth of 90 V is reached in 100 steps in a total time of about 1 s. The resulting electron plasma contains 3×10^9 particles and has a space charge of about 90 V. Although the presence of a buffer gas, similar to that used to trap positrons, increases the trapping rate, it was not used in the experiments here, since it causes significantly increased radial transport and resulting electron beam diameter.

There is evidence that elastic and inelastic collisions of electrons with vacuum impurity molecules cool the plasma to room temperature in a time of less than 1 s, analogous to the cooling observed for positron plasmas under similar conditions [23]. Besides cooling, background gas collisions produce radial transport on a time scale slightly longer than 1 s, which tends to broaden the radial distribution of the trapped plasma and reduce the total number of particles in the trap. After a 1 s store time, the diameter of the extracted electron beam is still largely unaffected by the background gas, and was measured to be 3.1 mm FWHM.

The large number of electrons in the trap (3×10^9, as compared to 10^7 positrons) creates a space charge, which can distort the potential near the exit gate electrode and lead to large uncertainties in the resulting beam energy. The modified exit gate electrode design shown in Fig. 4 increases the separation between the charge cloud and the exit gate and thereby decouples the extracted beam energy from the number of particles stored in the trap. A self-consistent Poisson–Boltzmann calculation, which includes the modified electrode geometry in the presence of the electron plasma, confirmed that the plasma potential has a negligible effect on the resulting beam energy.

It is difficult to measure the energy distribution of an electron beam in a magnetic environment with a retarding potential energy analyzer. In particular, when the beam is partially reflected by the analyzer electrode, the reflected particles interact with the original beam, causing a space charge build up, which can lead to irreproducible results. To reduce the magnitude of the beam–plasma interaction, the retarding energy analyzer was only raised for a short time (~10 μs) and then lowered to release any charge build up. This insures that no measurable space charge effects can occur. One advantage of this method is that the entire energy distribution can be measured during a single beam dump by a series of repeated raising and lowering of the retarding electrode. With each step, the re-

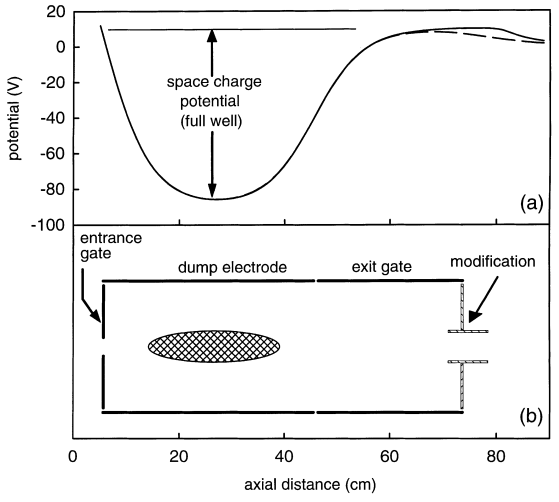

Fig. 4. (a) The axial potential distribution in the empty trap. (b) A schematic drawing of the electrode configuration. An electrode added into the electrode structure (shown in hash) gives rise to the potential depicted by the solid line. The dashed line was calculated without the modified electrode in place. The approximate position of the electron plasma is shown in (b).

tarding potential is increased allowing the entire beam distribution to be measured.

The axial energy distribution for an 0.1 μA electron beam was measured in this manner (cf. Fig. 5) and indicates an energy spread of 0.10 eV FWHM. Both experiment and potential calculation using a Poisson–Boltzmann solver (cf. Fig. 4) confirm that the absolute beam energy is set accurately by the externally applied exit gate potential. Larger beam current have also been generated and show a corresponding increase in the axial energy spread, e.g., a 1 μA electron beam has an energy spread of approximately 0.5 eV.

To achieve a fast turn-on of the electron beam, the waveform of the voltage applied to the dump electrode must be adjusted carefully. A simple, linear voltage ramp results in a rather slow current rise of over 1 ms (cf. Fig. 6(a)). Using an arbitrary waveform generator, a modified dump voltage waveform produces a much quicker turn-on (≈3 μs) and a longer flat-topped region of the electron beam (Fig. 6(b)). The total charge dumped from the well at any given time during beam extraction depends only on the dump voltage at that time. Therefore, the time-integrated current (i.e. total charge) waveform resulting from a linearly ramped dump waveform can be used conveniently as an inverse lookup table to find the dump voltage required to achieve an arbitrary current waveform.

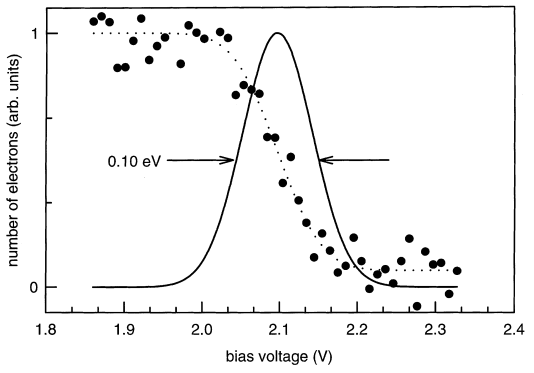

Fig. 5. Energy distribution of a 0.1 μA quasi steady-state electron beam. Filled circles are measured data, and the dashed line is an error function fit to the data. The solid line, which represents the energy distribution, is the derivative of the fit.

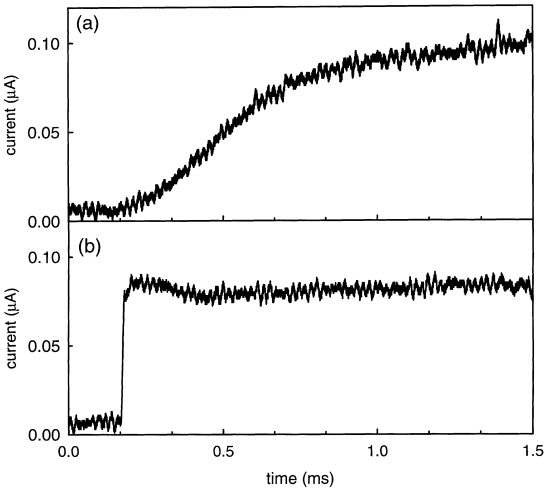

Fig. 6. (a) Current waveform of an electron beam obtained using a linear voltage ramp to dump the plasma. (b) Current waveform using an optimized dump voltage waveform to dump the plasma. Note the much faster turn-on (≈ 3 μs) and extended flat-topped region.

4. Conclusion

We have shown that room-temperature plasmas stored in Penning traps can be used as versatile sources of pulsed and steady-state beams of positrons and electrons. In the case of positrons, we measured an energy spread of 0.018 eV for both pulsed and quasi steady-state beams. Electron beams were extracted from a plasma of 3×10^9 particles. At a current of 0.1 μA, beam durations of ≈5 ms are achievable with an energy spread of 0.10 eV. It is likely that the performance of these cold, bright, electron and positron beam sources can be further improved by relatively straight forward modifications of the techniques described above.

Acknowledgements

The authors would like to acknowledge expert technical assistance from Eugene Jerzewski. This work is supported by the Office of Naval Research under Grant No. N00014-96-10579 and by the National Science Foundation under Grant No. PHY-9600407.

References

[1] S.J. Gilbert, C. Kurz, R.G. Greaves, C.M. Surko, Appl. Phys. Lett. 70 (1997) 1944.
[2] P.J. Schultz, K.G. Lynn, Rev. Mod. Phys. 60 (1988) 701.
[3] A.P. Mills, Jr., Science 218 (1982) 335.
[4] R. Suzuki, Y. Kobayashi, T. Mikado, H. Ohgaki, M. Chiwaki, T. Yamazaki, Hyperfine Interactions 84 (1994) 345.
[5] W.S. Crane, A.P. Mills, Jr., Rev. Sci. Instrum. 56 (1985) 1723.
[6] A.P. Mills, Jr., E.D. Shaw, R. Chichester, D.M. Zuckerman, Rev. Sci. Instrum. 60 (1989) 825.
[7] E. Ottewitte, A.H. Weiss (Eds.), AIP Conference Proceedings, vol. 303, American Institute of Physics, New York, 1992.
[8] M. Charlton, G. Laricchia, Hyperfine Interactions 76 (1993) 97.
[9] A.P. Mills, Jr., E.M. Gullikson, Appl. Phys. Lett. 49 (1986) 1121.
[10] E.M. Gullikson, A.P. Mills Jr., W.S. Crane, B.L. Brown Phys. Rev. B 32 (1985) 5484.
[11] B.L. Brown, W.S. Crane, A.P. Mills, Jr., Appl. Phys. Lett. 48 (1986) 739.
[12] D.A. Fischer, K.G. Lynn, D.W. Gidley, Phys. Rev. B 33 (1986) 4479.
[13] D.J. Wineland, C.S. Weimer, J.J. Bollinger, Hyperfine Interactions 76 (1993) 115.
[14] C.M. Surko, M. Leventhal, A. Passner, Phys. Rev. Lett. 62 (1989) 901.
[15] R.G. Greaves, M.D. Tinkle, C.M. Surko, Phys. Plasmas 1 (1994) 1439.
[16] A.P. Mills, Jr., Appl. Phys. 23 (1980) 189.
[17] G. Hart, J.M. Curtis, B.G. Peterson, Bull. Am. Phys. Soc. 41 (1996) 1523.
[18] D.L. Eggleston, C.F. Driscoll, B.R. Beck, A.W. Hyatt, J.H. Malmberg, Phys. Fluids B 4 (1992) 3432.
[19] D. Segers, J. Paridaens, M. Dorikens, L. Dorikens-Vanpraet, Nucl. Instr. and Meth. A 337 (1994) 246.
[20] X.-P. Huang, F. Anderegg, E.M. Hollmann, C.F. Hollmann, T.M. O'Neil, Phys. Rev. Lett., in press.
[21] L. Jong-Liang, J. Yates, J. Vac. Sci. Technol. A 12 (1994) 2795.
[22] C. Kuyatt, J. Sympson, Rev. Sci. Instrum. 38 (1967) 103.
[23] C. Kurz, R.G. Greaves, C.M. Surko, Phys. Rev. Lett. 77 (1996) 2929.